*Int. J. Electrochem. Sci.*, 17 **(2022)** Article Number: 221227, doi: 10.20964/2022.12.37

International Journal of
ELECTROCHEMICAL
SCIENCE
www.electrochemsci.org

# Investigation of transition metal (Fe, Ni, Co) complexes based on 1,10- phenanthroline as electrocatalysts for hydrogen evolution reaction

*Afaf A. Alrashedi, Fahad Abdulaziz, Khalaf M. Alenezi*

Department of Chemistry, College of Science, University of Ha'il, 81451, Kingdom of Saudi Arabia
*E-mail: k.alenezi@uoh.edu.sa

*Received:* 20 June 2022 / *Accepted:* 12 September 2022 / *Published:* 30 November 2022

Hydrogen production with zero carbon emission is considered as an excellent alternative to fossil fuels. To realize this goal, the design, and development of a new electrocatalyst is much needed. In the present work, we report electrochemical properties and hydrogen evolution reaction (HER) performance of three transition metal (M = Fe, Ni, Co) complexes based on 1,10- phenanthroline ligand. As compared to free acid (Ep = -1.85 V *vs* Ag/AgCl), electrocatalytic reduction of acetic acid takes place at lower overpotential (-1.22 to -1.50 V *vs* Ag/AgCl) in $[Bu_4N][BF_4]$-DMF electrolyte at room temperature. Based on the data obtained and earlier reports, a possible mechanism of HER has also been delineated.

**Keywords:** Hydrogen evolution reaction, Electrocatalysis, Tris(1,10-phenanthroline), Potential shifting, Diffusion coefficient.

## 1. INTRODUCTION

In the last few decades, the demand for fossil fuels increased tremendously leading rise in greenhouse gases and environmental deterioration [1]. Besides, the depletion of fossil resources is accelerating day by day, leading to an increase in their cost and burden on the government. To tackle the issues, researchers across the globe are working together to find a clean, renewable alternative source to fossil fuels [2]. Nowadays, the hydrogen economy has gained tremendous interest as it has the potential to serve as the main source of energy in the future. Hydrogen has many properties that make it suitable to be an alternative source of energy, it has the highest gravimetric energy density among all chemical fuels (142 MJ $kg^{-1}$) [3,4]. Hydrogen is a clean fuel and clean energy carrier without toxic emissions especially ($CO_2$) and can be used for electricity generation be applied in fuel cells [5]. By 2030, if the hydrogen production technology receives high support from the government and developed by researchers, so the use of crude oil and coal will reduce to 40.5% and 36.7%, respectively [6].

Electrocatalytic hydrogen evolution reaction (HER) is an electrochemical process where redox reactions occur between electrode and electrolyte interface and $H_2$ is generated by reducing proton ($H^+$) [3]. Despite this process of HER is intriguing, a suitable electrocatalyst is required to make this process feasible and economical. Undoubtedly several electrocatalysts are available, most of them are based on costly metals such as platinum. In the quest of cheaper, abundant, and alternative, researchers evaluated catalysts based on first row transition metals such as Fe, Co, and Ni [7, 8]. It is to be noted that the selection of the ligand is very crucial, as a change in the oxidation state may be accompanied by a change in the geometry around the metal center [8]. Based on this, a plethora of stable complexes with chelating bidentate ligands such as 2,2-bipyridine, 1,10-phenanthroline (phen) and their derivatives have been reported [9]. Especially, Phen-based complexes are particularly interesting due to their high rigidity, planarity, aromaticity, hydrophobicity, and stability [9–11]. The excellent electronic features of phen exemplified by their electron deficiency giving rise to a great acceptor which stabilize the metal center of the complex. Phen-based complexes are used in many applications including binding agent and cleaving reagent for biomolecules [12,13].

Owing to the potential future of HER and the unique properties of phen, we present herein the electrochemical properties and hydrogen evolution reaction (HER) performance of three transition metal (M = Fe, Ni, Co) complexes based on phen ligand (Fig.1). We found that these complexes show excellent activity under normal conditions. The results of the findings are discussed herein.

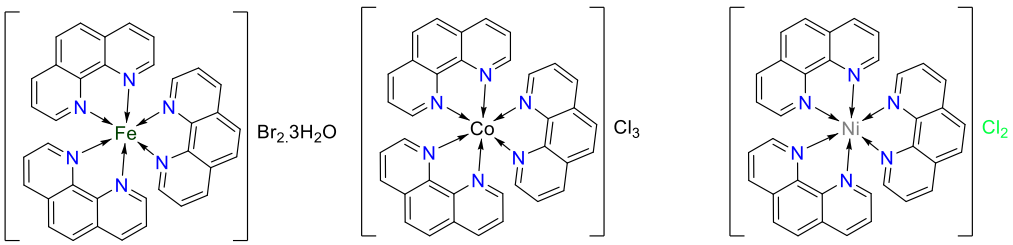


**Figure 1**. General structure of the complexes (a) $[Fe(phen)_3]Br_2.3H_2O$, (b) $[Co(phen)_3]Cl_3$ and (c) $[Ni(phen)_3]Cl_2$.

## 2. EXPERIMENTAL DETAILS

The complexes $[Fe(phen)_3]Br_2.3H_2O$, $[Co(phen)_3]Cl_3$, and $[Ni(phen)_3]Cl_2$ were synthesized according to the previously described procedures [14–16]. Acetic acid ($CH_3COOH$) and Dimethylformamide (DMF) were purchased from Sigma Aldrich. Each complex prepared separately for the HER experiment. In a typical experiment, 0.03 g of the complexes were added to the electrochemical cell. This is followed by the addition of 15 mL of DMF and 0.2 M electrolyte tetrabutylammonium tetrafluoroborate $[NBu_4][BF_4]$. The solutions were purged with nitrogen gas to remove dissolved oxygen. A conventional three-electrode system containing a vitreous carbon as working (0.07 $cm^2$), a platinum wire as auxiliary and Ag/AgCl as a reference electrode was used. Cyclic voltammetry (CV) experiments were carried out on Autolab PGSTAT 128 potentiostat. 1.0 mL of $CH_3COOH$ was dissolved

in 10 mL of DMF and different concentrations (0.58 mM, 1.16 mM, 1.75 mM, 2.33 mM, 2.91 mM, 3.50 mM, 4.08 mM, 4.66 mM, 5.25 mM, 5.83 mM, 6.41 mM) were added during the experiment.

## 3. RESULT AND DISCUSSION

### *3.1 Electrochemical studies of the complexes*

The electrochemical response of (0.03 g, 2.8 mM) of $[Co(phen)_3]Cl_3$, (0.03g, 2.5 mM) of $[Fe(phen)_3]Br_2.3H_2O$ and (0.03g, 2.9 mM) of $[Ni(phen)_3]Cl_2$ dissolved in DMF containing 0.2 M $[NBu_4][BF_4]$ at different scan rate is shown in Fig. 2.

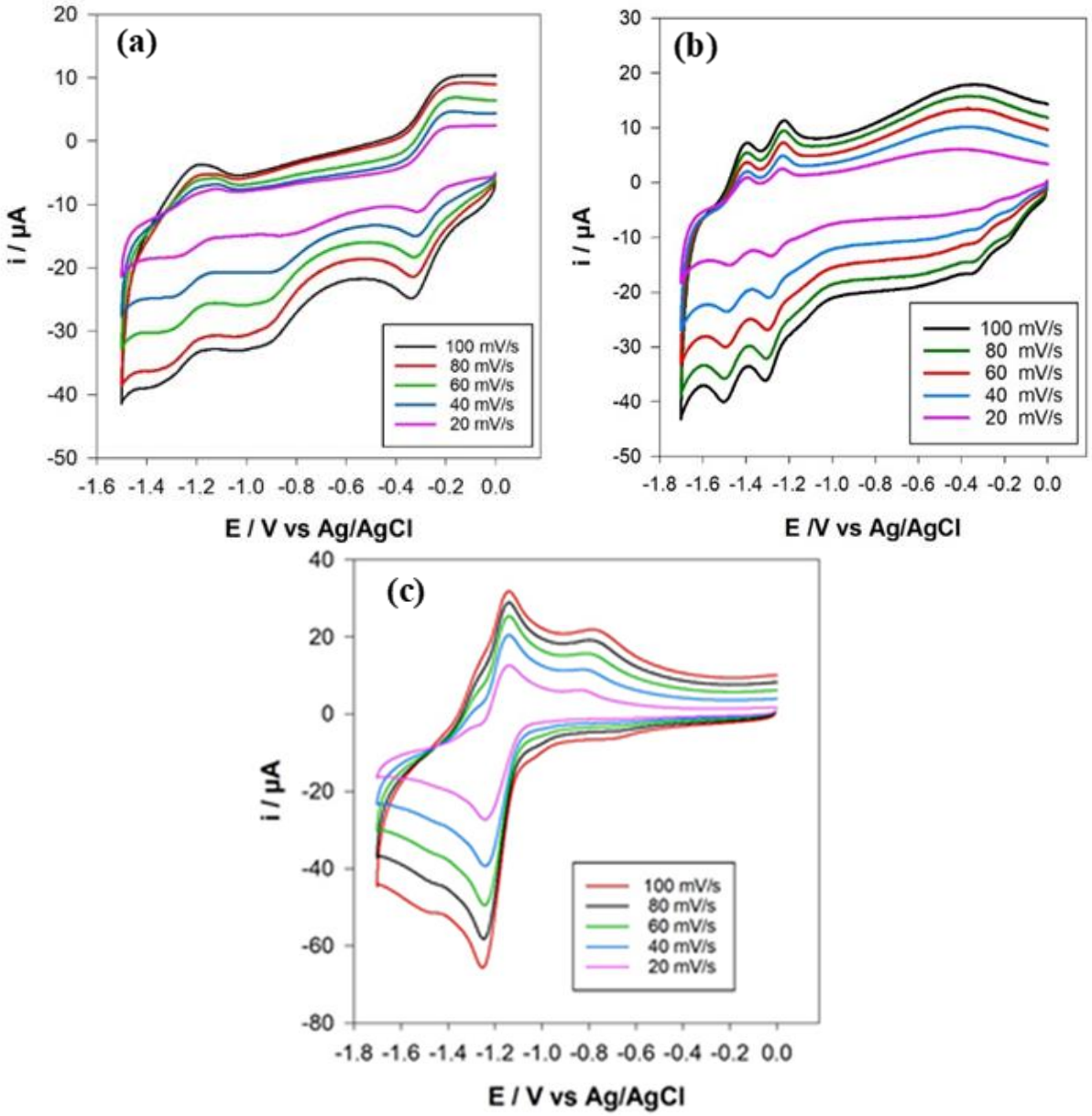


**Figure 2**: Cyclic voltammetry curve of (a) 2.8 mM of $[Co(phen)_3]Cl_3$, (b) 2.5 mM of $[Fe(phen)_3]Br_2.3H_2O$ and (c) 2.9 mM of $[Ni(phen)_3]Cl_2$ in 0.2 M $[NBu_4][BF_4]$ DMF-solution at carbon electrode with different scan rate under nitrogen.

From the figure, it is clear that Co(III) complex undergoes three successive reversible one-electron reduction at $E_p$= -0.32 V, -0.88 V and -1.30 V. These three peaks can be assigned to Co(III) → Co(II) → Co(I) → Co(0) couples, respectively. On the other hand, Fe(II) and Ni(II) complexes exhibit two-electron reduction at $E_p$= -1.30 V & -1.50 V and -1.25 V & -1.48 V, respectively attributed to M(III)→ M(II) → M(I) couples. Note that there is an additional peak at -0.33 V in case of Fe(II) complex, possibly due to impurity. Besides, the current varies linearly with the square root of the scan rate, demonstrating non-complicated mass transfer control (Figure 3).

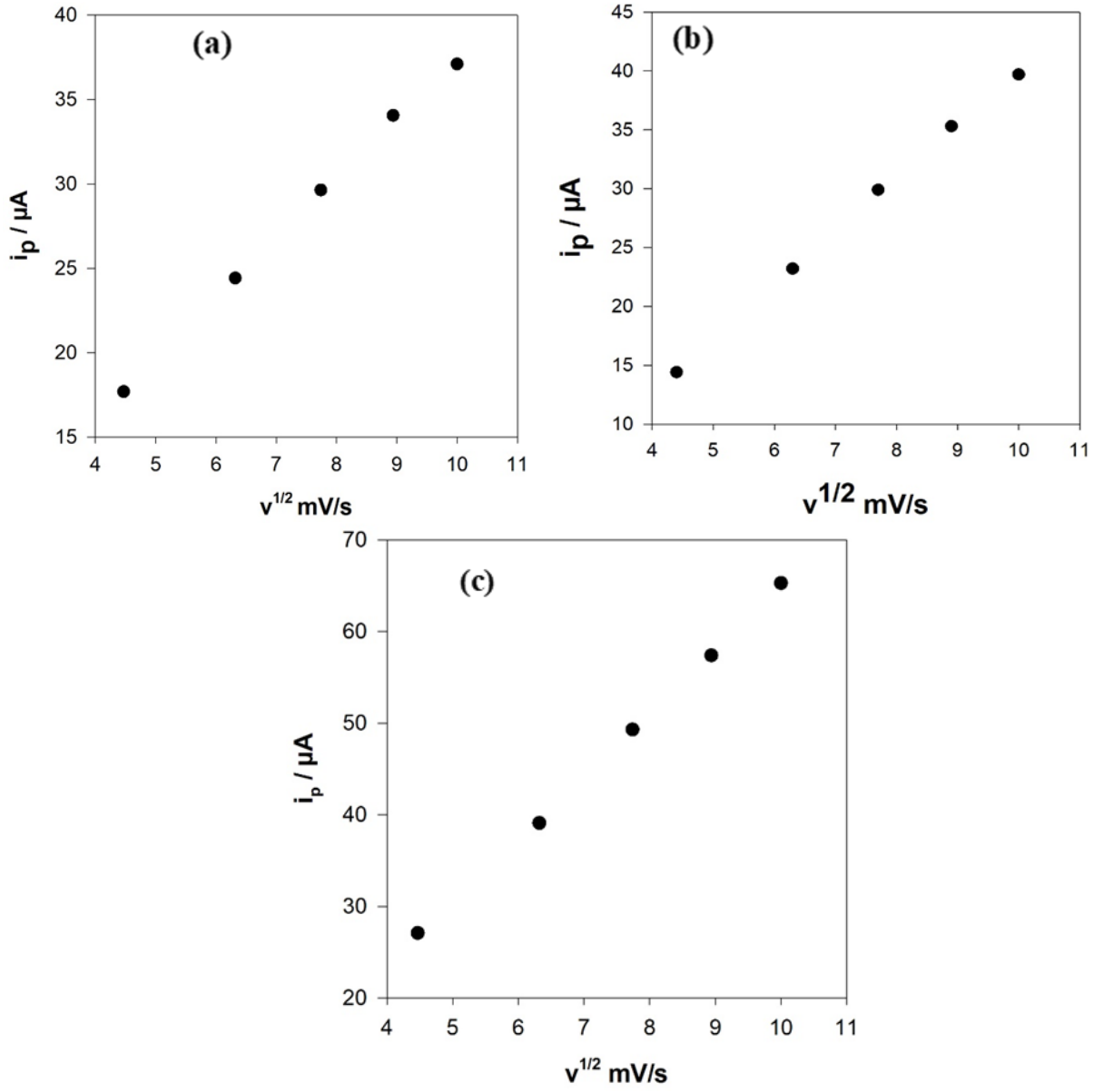


**Figure 3**. The relationship between square root of scan rate ($v^{1/2}$) and the peak current ($i_p$) for complexes (a)$[Co(phen)_3]Cl_3$, (b)$[Fe(phen)_3]Br_2.3H_2O$ and (c)$[Ni(phen)_3]Cl_2$

*3.2. Determination of diffusion coefficient*

The peak current, $i_p$, for a reversible couple (at 25 °C) is given by the Randles–Sevcik equation 1:

$$i_p = (2.69 \times 10^5)n^{3/2}ACD^{1/2}v^{1/2} \quad (1)$$

where n is the number of electrons, A the electrode area (in $cm^2$), C the concentration (in $mol/cm^3$), D the diffusion coefficient (in $cm^2/s$), and v the potential scan rate (in V/s) [17]. The diffusion coefficient at 20 mV/s scan rate is given in Table 1.

**Table 1.** Diffusion coefficient of reduced complexes at scan rate 20 mV/s.

| **Complex** | **$i_p$ (A)** | **Diffusion coefficient ($cm^2$ /s)** |
|---|---|---|
| $[Co(phen)_3]Cl_3$ | $-18.42\times10^{-6}$ A | $5.92\times10^{-3}$ $cm^2$ $s^{-1}$ |
| $[Fe(phen)_3]Br_2.3H_2O$ | $-15.3\times10^{-6}$ A | $5.33\times10^{-3}$ $cm^2$ $s^{-1}$ |
| $[Ni(phen)_3]Cl_2$ | $-27.4\times10^{-6}$ A | $1.48\times10^{-3}$ $cm^2$ $s^{-1}$ |

*3.3. Hydrogen evaluation reaction (HER) studies*

It is well established that the direct reduction of $CH_3COOH$ on vitreous carbon electrode takes place at $E_p$ = -1.85 V vs Ag/AgCl (Table 2). Fig. 4 depicts the electrocatalytic performance of the complexes $[Co(phen)_3]Cl_3$, $[Fe(phen)_3]Br_2.3H_2O$ and $[Ni(phen)_3]Cl_2$. The potential shifting for all complexes compared to the reduction of $CH_3COOH$ is given in Table 2. It is clear that the proton reduction takes place near the third peak in case of $[Co(phen)_3]Cl_3$ ($E_p$ = -1.22 V vs Ag/AgCl), while it takes place near the second peak in case of $[Fe(phen)_3]Br_2.3H_2O$ ($E_p$ = -1.50 V vs Ag/AgCl) and $[Ni(phen)_3]Cl_2$ ($E_p$ = -1.48V vs Ag/AgCl). The complex $[Co(phen)_3]Cl_3$ shifted the direct reduction of acid towards more positive potential (630 mV) as compared to $[Fe(phen)_3]Br_2.3H_2O$ and $[Ni(phen)_3]Cl_2$ (350 and 370 eV, respectively).

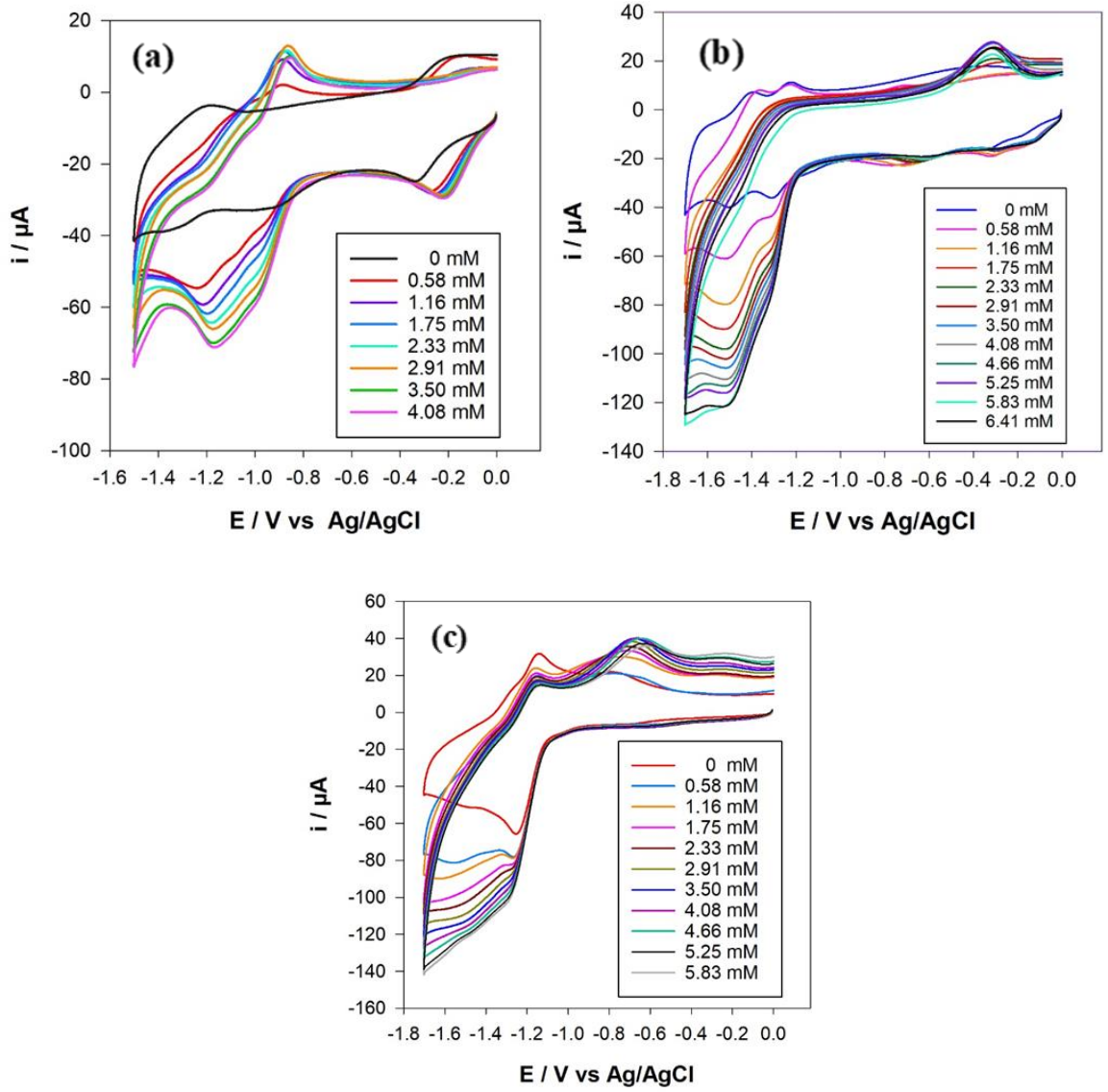


**Figure 4**. Cyclic voltammogram of (a) 2.8 mM of $[Co(phen)_3]Cl_3$, (b) 2.5 mM of $[Fe(phen)_3]Br_2.3H_2O$ and (c) 2.9 mM of $[Ni(phen)_3]Cl_2$ in 0.2 M $[NBu_4][BF_4]$ DMF-solution at scan rate 100 mv/s and different concentration of ($CH_3COOH$).

**Table 2.** Comparison between the reduction potential of $CH_3COOH$ and the potential shifting of each complex.

| **Reduction of $CH_3COOH$** | **Potential E /V vs Ag/AgCl** | **Shift / mV more positive** |
|---|---|---|
| Catalyst free | -1.85 V | - |
| $[Co(phen)_3]Cl_3$ | -1.22 V | 630 |
| $[Fe(phen)_3]Br_2.3H_2O$ | -1.50 V | 350 |
| $[Ni(phen)_3]Cl_2$ | -1.48V | 370 |

*3.3.2. Calculation of the rate constants ($k_{cat}$)*

The relationship between $i_{cat}/i_0$ and [$CH_3COOH$] at carbon electrode is given in Fig. 5. The peak current, $i_{cat}$ measured at 100 $mVs^{-1}$ after adding $CH_3COOH$ and $i_0$ is for the peak current for Co(I)/Co (0), Fe(I)/Fe (0) and Ni(I)/Ni(0) in the absence of acid at the same scan- rate. As it is clear from the figure, the current increases until it reach the highest electrocatalytic activities which were observed in the presence of 3.50 mM, 5.83 mM, and 5.25 mM for $[Co(phen)_3]Cl_3$, $[Fe(phen)_3]Br_2.3H_2O$ and $[Ni(phen)_3]Cl_2$, respectively.

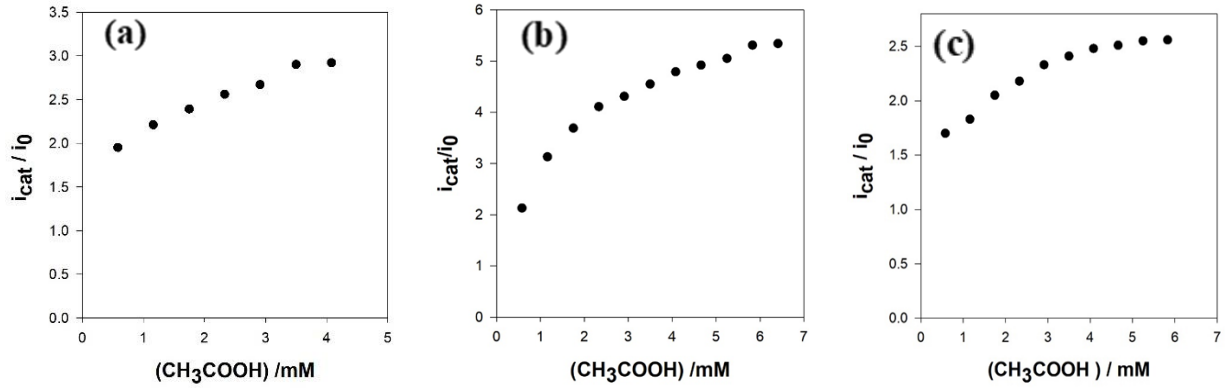


**Figure 5.** The effect of concentrations of acetic acid on $i_p/i_0$ ratio at carbon electrode contain (a) 2.8mM of $[Co(phen)_3]Cl_3$, (b) 2.5mM of $[Fe(phen)_3]Br_2.3H_2O$ and (c) 2.9mM of $[Ni(phen)_3]Cl_2$ in DMF solvent containing 0.2M$[NBu_4][BF_4]$.

The rate constants for all complexes were also calculated using equation (2) [18]:

$$k_{obs} = 0.1992(Fv/RTn^2)(i_p/i_0)^2 \qquad (2)$$

where F is the faraday constant, R is the gas constant, T is the temperature, $i_p$ is the peak catalytic current, $i_o$ is the peak current in the absence of acetic acid, v is scan rate and n is the number of electrons. The rate constants ($k_{cat}$, 25 °C) of the catalysis at glassy carbon electrode is shown in Table 3. We found that as the concentration of acid increases ,the potential shifting decrease until become constant (Fig. 6). Therefore, it can be concluded that for $[Co(phen)_3]Cl_3$ the potential shifting decrease until become constant at 2.91mM while in case of $[Fe(phen)_3]Br_2.3H_2O$ the potential shifting is decrease until become constant at 4.66 mM and for $[Ni(phen)_3]Cl_2$ the potential shifting is decrease until become constant at 5.25 mM.

**Table 3.** The rate constant ($k_{obs}$, 25 °C) for catalysis of the different electrocatalyst complexes.

| **Complex** | **$i_p/i_o$** | **Rate constant ($k_{obs}$) / $s^{-1}$** |
|---|---|---|
| $Co(phen)_3]Cl_3$ | 2.90 | 6.52 |
| $[Fe(phen)_3]Br_2.3H_2O$ | 5.31 | 21.86 |
| $[Ni(phen)_3]Cl_2$ | 2.55 | 5.04 |

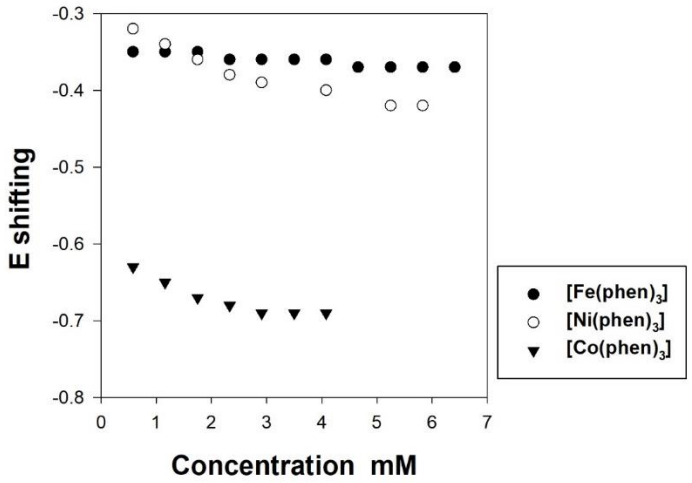


**Figure 6.** The effect increasing of concentrations of acetic acid on potential shifting at carbon electrode contain (a) 2.8 mM of $[Co(phen)_3]Cl_3$, (b) 2.5mM of $[Fe(phen)_3]Br_2.3H_2O$ and (c) 2.9 mM of $[Ni(phen)_3]Cl_2$ in DMF solvent containing 0.2M $[NBu_4][BF_4]$.

Table 4 compares the reductional potential of various catalysts under different conditions. It is well known that the shift in potential is the function of ligand, complex, and proton source selected. Using these parameters potential can be fine-tuned. In this study, we found that compared to earlier reported Fe and Ni complexes [19-22], our complexes showed larger shift in the potential.

**Table 4.** Reductional potential of various catalysts under different conditions

| **Complex** | **Proton source** | **The potential of catalyst-free direct reduction (V)** | **Potential for reduction of acid in the presence of a catalyst** | **Potential shifting (mV)** | **Condition** | **Ref.** |
|---|---|---|---|---|---|---|
| $[Co(phen)_3]Cl_3$ | $CH_3COOH$ | -1.85 Ag/AgCl | -1.22 V Ag/AgCl | 630 | $[NBu_4][BF_4]$ –DMF | Current work |
| $[Fe(phen)_3]Br_2.3H_2O$ | $CH_3COOH$ | -1.85 Ag/AgCl | -1.50 V Ag/AgCl | 350 | | |
| $[Ni(phen)_3]Cl_2$ | $CH_3COOH$ | -1.85 Ag/AgCl | -1.48 V Ag/AgCl | 370 | | |
| Co(TFPP) | $CH_3COOH$ | -1.81 $Ag/AgNO_3$ | -1.45 V $Ag/AgNO_3$ | 360 | $[NBu_4]ClO_4$–DMF | [19] |
| $[Co(PLSC)(SO_4)(H_2O)_2]$ | $CH_3COOH$ | -1.85 Ag/AgCl | -1.58 V Ag/AgCl | 270 | $[NBu_4][BF_4]$ –DMF | [20] |
| Mn(TPP)Cl | $Et_3NHCl$ | -.1.60 Ag/AgCl | -1.2 V Ag/AgCl | 400 | [NBu4][BF4]-ACN | [21] |
| Fe(PFTPP)Cl | TEA | -1.6 Ag/AgCl | -1.3 V Ag/AgCl | 300 | $[NBu_4][BF_4]$–ACN | [22] |
| $CH_3COOH$ = Acetic acid, DMF = Dimethylformamide, TEA = Triethylamine, ACN = Acetonitrile, ($Et_3NHCl$) = triethylamine hydrochloride | | | | | | |

*3.4. Possible mechanism of HER*

A typical HER in acidic media usually takes place in three steps. The first step is the Volmer step in which electrochemical adsorption of hydrogen and reduction takes place. This is followed by

Heyrovsky step, i.e., electrochemical desorption. Finally Tafel reaction (chemical desorption) takes place with the generation of molecular hydrogen. [23] Based on this information and earlier reports, we propose the the following mechanism of HER reaction (Scheme 1a & b). [3,24] In case of Co(III), succecive $3e^-$ reduction of complex formed an active species Co(0) which upon oxidative protonation formed hydride complex (Scheme 1a). This reacted with another proton to generate Co(II) intermediate and molecular hydrogen. From the data obtained, it is clear that HER takes place near the second peak in case of Fe(II) and Ni(II) complexes. In this case too, $2e^-$ reduction led to the formation of active species M(0) which then undergoes oxidative protonation and protonolysis to release molecular hydrogen and regenrate the catalyst (Scheme 1b).

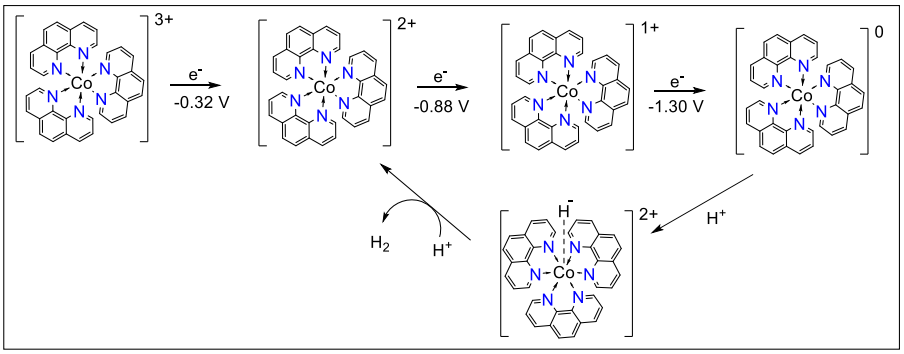


(a)

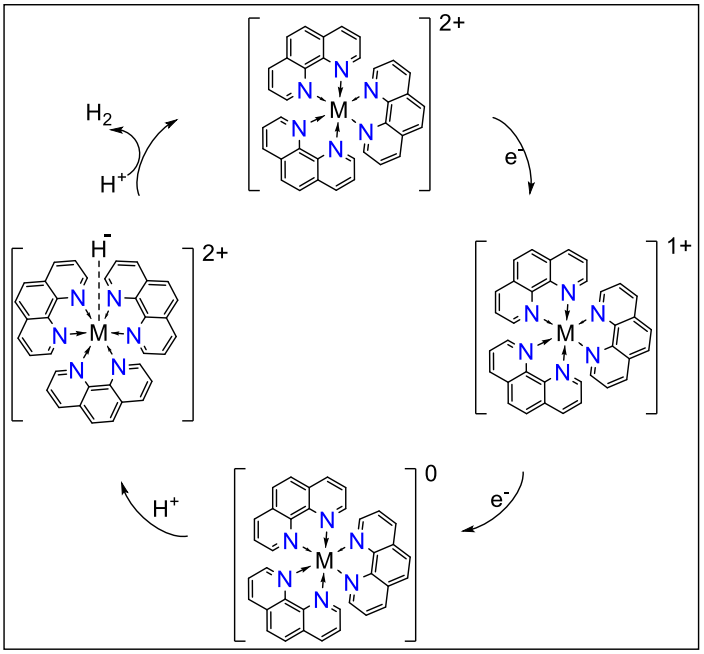


(b)

**Scheme 1**. Possible mechanism of HER by (a) Co(III) complex and (b) M(II) (where M = Fe, Ni) complexes.

## 4. CONCLUSION

Electrocatalytic HER is an electrochemical process where $H_2$ is generated by reducing protons ($H^+$). The electrocatalytic performance of the complex $[Co(phen)_3]Cl_3$ was observed for the proton

reduction for [Co (phen)$_3$]Cl$_3$ at $E_p$ = -1.22 V vs Ag/AgCl while in case of [Fe (phen)$_3$]Br$_2$.3H$_2$O at $E_p$ = -1.50 V vs Ag/AgCl and for [Ni(phen)$_3$]Cl$_2$ was at $E_p$ = -1.48V vs Ag/AgCl. The complex [Co(phen)$_3$]Cl$_3$ was shifted to more positive potential value (630 mV) than other complexes. In addition, the current is increases until it reach to the highest electrocatalytic activities in the presence of 3.50 mM, 5.83 mM and 5.25 mM for [Co(phen)$_3$]Cl$_3$, [Fe(phen)$_3$]Br$_2$.3H$_2$O and [Ni(phen)$_3$]Cl$_2$ , respectively. We also prposed a possible mechanism for all complexes for hydrogen production.

## References


1. M. Yusuf, *Orient. J. Phys. Sci.*, 6 (2022) 32–35.
2. X. Zou, Y. Zhang, *Chem. Soc. Rev.*, 44 (2015) 5148–5180.
3. G. Zhao, K. Rui, S.X. Dou, W. Sun, *Adv. Funct. Mater.*, 28 (2018) 1–26.
4. M. Momirlan, T.N. Veziroglu, *Int. J. Hydrogen Energy*, 30 (2005) 795–802.
5. S.E. Hosseini, M.A. Wahid, *Renew. Sustain. Energy Rev.*, 57 (2016) 850–866.
6. J.X.W. Hay, T.Y. Wu, J.C. Juan, J. Md. Jahim, *Biofuels, Bioprod. Biorefining*, 7 (2013) 334–352.
7. J. Wang, X. Yue, Y. Yang, S. Sirisomboonchai, P. Wang, X. Ma, A. Abudula, G. Guan, *J. Alloys Compd.*, 819 (2020) 153346.
8. M.J. Celestine, M.A.W. Lawrence, O. Schott, V. Picard, G.S. Hanan, E.M. Marquez, C.G. Harold, C.T. Kuester, B.A. Frenzel, C.G. Hamaker, S.E. Hightower, C.D. McMillen, A.A. Holder, *Inorganica Chim. Acta*, 517 (2020).
9. D.E. Arthur, I.U. Nkole, C.R. Osunkwo, *Chem. Africa*, 4 (2021) 63–69.
10. A. Bencini, V. Lippolis, *Coord. Chem. Rev.*, 254 (2010) 2096–2180.
11. H.G. Bonacorso, R. Andrighetto, C.P. Frizzo, N. Zanatta, M.A.P. Martins, *Targets Heterocycl. Syst.*, 19 (2015) 1–27.
12. G. Yahioglu, P. Sammes, *Chem. Soc. Rev.*, 23 (1994) 327–344.
13. K.E. Erkkila, D.T. Odom, J.K. Barton, *Chem. Rev.*, 99 (1999) 2777–2795.
14. G. Grassini-Strazza, S. Isola, *J. Chromatogr. A*, 154 (1978) 122–126.
15. V.E. Berkheiser, M.M. Mortland, *Clays Clay Miner.*, 25 (1977) 105–112.
16. G. Grassini-Strazza, M. Sinibaldi, A. Messina, *Inorganica Chim. Acta*, 44 (1980) 295–297.
17. J. Wang, Analytical Electrochemistry, third, John Wiley & Sons, Inc, (2006) Hoboken, New Jersey.
18. T. Liu, D.L. Dubois, R.M. Bullock, *Nat. Chem.*, 5 (2013) 228–233.
19. D.X. Zhang, H.Q. Yuan, H.H. Wang, A. Ali, W.H. Wen, A.N. Xie, S.Z. Zhan, H.Y. Liu, *Transit. Met. Chem.*, 42 (2017) 773–782.
20. V. Jevtovic, K.M. Alenezi, H. El Moll, A. Haque, S.A. Al-Zahrani, J. Humaidi, D. Vidovic, *J. Chem. Soc. Pakistan*, 43 (2021) 673–681.
21. K. Alenezi, *J. New Mater. Electrochem. Syst.*, 20 (2017) 43–47.
22. K. Alenezi, *Int. J. Electrochem. Sci.*, 12 (2017) 812–818.
23. C. Wang, S. Yang, Y. Chen, *J. Appl. Electrochem.* (2019) 539–550.
24. W. Zhang, W. Lai, R. Cao, *Chem. Rev.*, 117 (2017) 3717–3797.